

A Study of Gas Flow in a Slurry Bubble Column Reactor for the DME Direct Synthesis: Mathematical Modeling from Homogeneity vs. Heterogeneity Point of View

Mohammad Kazemeini^{*1}, Moslem Fattahi² and Leila Vafajoo³

¹Department of Chemical and Petroleum Engineering, Sharif University of Technology, Azadi Avenue, Tehran, Iran

²Department of Chemical Engineering, Abadan Faculty of Petroleum Engineering, Petroleum University of Technology, Abadan, Iran

³Chemical & Environmental Engineering Group, Graduate Faculty of Engineering, Islamic Azad University, South Tehran Branch. Tehran, Iran

(Received 1 December 2014, Accepted 16 December 2014)

Abstract

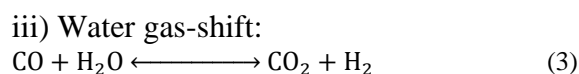
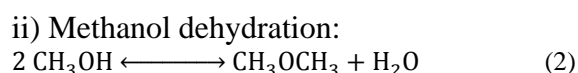
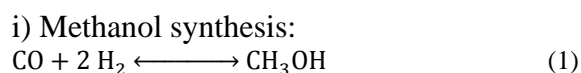
In the present study, a heterogeneous and homogeneous gas flow dispersion model for simulation and optimization of a large-scale catalytic slurry reactor for the direct synthesis of dimethyl ether (DME) from synthesis gas (syngas) and CO₂, using a churn-turbulent regime was developed. In the heterogeneous flow model, the gas phase was distributed into two bubble phases including small and large while in the homogeneous one, the gas phase was distributed into only one large bubble phase. The results indicated that the heterogeneous gas flow model was in a better agreement with experimental pilot-plant data compared with that of the homogeneous one. Also, through investigating the heterogeneous gas flow for small bubbles as well as the large bubbles in the slurry phase (*i.e.*; including paraffins and the catalyst), the temperature profile along the reactor was obtained. The optimum value of reactor diameter and height obtained at 3.2 and 20 meters respectively. The effects of operating variables on the axial catalyst distribution, DME productivity and CO conversion were also understudied in this research.

Keywords: Dimethyl ether synthesis, Homogeneous and heterogeneous gas flow, Modelling, Slurry bubble column

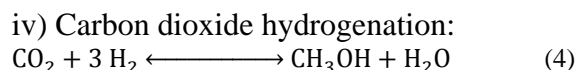
Introduction

Dimethyl ether (DME) is a clean, colourless, easily liquefied and transported material. It has remarkable potential for increased use as an automotive fuel, electric power generator and utilized in domestic applications such as heating and cooking. Moreover, it is a good substitute for the liquefied petroleum gas (LPG), transportation fuel, propellants and chemical feedstock [1]. It is produced from a variety of feed-stocks such as natural gas, crude oil, residual oil, coal, waste products as well as biomass [2]. It might be manufactured directly from synthesis gas produced by the gasification of coal and biomass or through natural gas reforming and indirectly via methanol dehydration reaction [2]. Reactions associated with the single-stage process for the DME

production may be divided into the following steps:



and



Synthesis of the DME in a single step following the syngas to DME conversion process (STD) on a bifunctional catalyst has advantages over the two-step process (*i.e.*;

synthesis of methanol and dehydration of it to DME). This process due to the lower thermodynamic limitations imposed upon the methanol synthesis allows the process to be carried out at higher temperatures and lower pressures [3]. This thermodynamic advantage helps the incorporation of CO₂ as a co-feed with the syngas, or the transformation of (H₂+CO₂) into the DME. Considerable attention has been paid in the literature to the use of CO₂ as a raw material in the synthesis of chemicals and liquid energy carriers in order to mitigate the accumulation of CO₂ in the atmosphere [4]. Amongst the different alternatives, the synthesis of DME is an interesting route to combine and upgrade (via gasification) of alternative sources to oil, particularly lignocellulosic biomass, with large-scale CO₂ sequestration [5,6]. A good performance of the catalyst has already been proven [7,8], and CuO-ZnO-Al₂O₃ and γ -Al₂O₃ functions are considered in the literature as the more suitable metallic and acid functions for the synthesis of methanol and its dehydration to DME, respectively [9,10]. It should be noted that, a catalyst prepared with excess acid function helps to understand the kinetic results conditioned by the metallic function. Consequently, deactivation is a result of coke deposition on the metallic function [11]. This idea has been quantified by including a deactivation equation in the kinetic model [12]. The use of excess acid function in the catalyst enhances its stability through avoiding the acid function deactivation upon product distribution. This is advantageous for the use of this catalyst in industrial scale. It has also been proven that the catalyst fully recovers its kinetic performance when used in reaction-regeneration cycles, in which the coke is burnt out with air at a temperature below 325°C [13].

There are several researches available in the literature performed upon mathematical modeling of the DME production through different reactors. Fazlollahnejad and co-workers investigated methanol dehydration in a bench scale adiabatic fixed bed reactor,

experimentally [14]. They investigated the effects of weight hourly space velocity and temperature upon methanol conversion. Farsi *et al.* modeled and simulated an industrial DME fixed bed reactor under dynamic conditions [15]. They investigated the stability and controllability of the DME reactor through dynamic simulation under a conventional feedback PID controller. These researchers analyzed steady state operability characteristics of a conventional DME reactor using the framework of Vinson and Georgakis procedure [16]. Since industrial plants have large capacities, the investment cost of such plants is rather high. Therefore, any small enhancement in the process could yield significant financial rewards. Moreover, operating of the DME plant under optimal conditions reduces operational costs and enhances process efficiency hence, economic benefits are due. Farsi *et al.* proposed and optimized an isothermal reactor to produce DME from the methanol dehydration [17]. The simulation results showed that, the isothermal reactor is more efficient compared to the more traditional adiabatic reactor. Farsi and Jahanmiri modeled and optimized a water cooled membrane fixed bed reactor to produce DME under the steady state condition [18]. Water vapor removal from the reaction zone in the membrane reactor yields lower water concentration over the catalyst pellets and leads to higher catalyst lifetime and lower purification cost. Omata *et al.* studied DME production from syngas in a temperature gradient reactor to overcome thermodynamic equilibrium limitations [19]. Then, they optimized the operating conditions of the reactor to enhance the CO conversion through combined genetic algorithm and neural network. Kordabadi and Jahanmiri modeled and optimized methanol synthesis reactor under the steady state condition [20]. They obtained the optimal temperature profile along the reactor to maximize methanol production rate.

Table 1: Homogeneous and heterogeneous gas flow models in a slurry bubble column

Homogeneous gas flow model	Heterogeneous gas flow model
<p>Mass balance for Gas phase</p> $\frac{\partial}{\partial z} \left[\varepsilon_G E_G \frac{\partial C_{j,G}}{\partial z} \right] - \frac{\partial (U_G C_{j,G})}{\partial z} - k_1 a (C_j^* - C_{j,SL}) = 0$ <p>Mass balance for slurry phase</p> $\begin{aligned} \frac{\partial}{\partial z} \left[(1 - \varepsilon_G) E_{SL} \frac{\partial C_{j,SL}}{\partial z} \right] - \frac{\partial (U_{SL} C_{j,SL})}{\partial z} \\ + k_1 a_{LB} (C_j^* - C_{j,SL}) \\ + k_1 a_{sb} (C_j^* - C_{j,SL}) + (1 \\ - \varepsilon_G) \sum_{i=1}^{N_r} M_{cat} v_{j,i} r_i = 0 \end{aligned}$ <p>Mass balance for particles</p> $\frac{\partial}{\partial z} \left[(1 - \varepsilon_G) E_S \frac{\partial C_S}{\partial z} \right] - \frac{\partial}{\partial z} [(1 - \varepsilon_G) U_P - U_{SL}] C_S = 0$ <p>Boundary condition in the inlet of column</p> $\begin{aligned} U_G C_{j,G} - \varepsilon_G E_G \frac{\partial C_{j,G}}{\partial z} &= U_G C_{j0} \\ U_{SL} C_{j,SL} - (1 - \varepsilon_G) E_{SL} \frac{\partial C_{j,SL}}{\partial z} &= 0 \\ (1 - \varepsilon_G) E_S \frac{\partial C_S}{\partial z} + ((1 - \varepsilon_G) U_P - U_{SL}) C_S \\ + U_{SL} C_{ave} &= 0 \end{aligned}$ <p>Boundary condition in the outlet of column</p> $\frac{\partial C_{j,G}}{\partial z} = 0, \frac{\partial C_{j,SL}}{\partial z} = 0, \frac{\partial C_S}{\partial z} = 0$	<p>Mass balance for Large-bubbles phase</p> $\frac{\partial}{\partial z} \left[\varepsilon_{LB} E_{LB} \frac{\partial C_{j,LB}}{\partial z} \right] - \frac{\partial (U_{LB} C_{j,LB})}{\partial z} - k_1 a_{LB} (C_j^* - C_{j,SL}) = 0$ <p>Mass balance for Small-bubbles phase</p> $\frac{\partial}{\partial z} \left[\varepsilon_{SB} E_{SB} \frac{\partial C_{j,SB}}{\partial z} \right] - \frac{\partial (U_{SB} C_{j,SB})}{\partial z} - k_1 a_{SB} (C_j^* - C_{j,SL}) = 0$ <p>Mass balance for slurry phase</p> $\begin{aligned} \frac{\partial}{\partial z} \left[(1 - \varepsilon_G) E_{SL} \frac{\partial C_{j,SL}}{\partial z} \right] - \frac{\partial (U_{SL} C_{j,SL})}{\partial z} \\ + k_1 a_{LB} (C_j^* - C_{j,SL}) \\ + k_1 a_{sb} (C_j^* - C_{j,SL}) + (1 \\ - \varepsilon_G) \sum_{i=1}^{N_r} M_{cat} v_{j,i} r_i = 0 \end{aligned}$ <p>Mass balance for particles</p> $\frac{\partial}{\partial z} \left[(1 - \varepsilon_G) E_S \frac{\partial C_S}{\partial z} \right] - \frac{\partial}{\partial z} [(1 - \varepsilon_G) U_P - U_{SL}] C_S = 0$ <p>Boundary condition in the inlet of column</p> $\begin{aligned} U_{LB} C_{j,LB} - \varepsilon_{LB} E_{LB} \frac{\partial C_{j,LB}}{\partial z} &= U_{LB} C_{j0} \\ U_{SB} C_{j,SB} - \varepsilon_{SB} E_{SB} \frac{\partial C_{j,SB}}{\partial z} &= U_{SB} C_{j0} \\ U_{SL} C_{j,SL} - (1 - \varepsilon_G) E_{SL} \frac{\partial C_{j,SL}}{\partial z} &= 0 \\ (1 - \varepsilon_G) E_S \frac{\partial C_S}{\partial z} + ((1 - \varepsilon_G) U_P - U_{SL}) C_S + U_{SL} C_{ave} \\ &= 0 \end{aligned}$ <p>Boundary condition in the outlet of column</p> $\frac{\partial C_{j,LB}}{\partial z} = 0, \frac{\partial C_{j,SL}}{\partial z} = 0, \frac{\partial C_{j,SB}}{\partial z} = 0, \frac{\partial C_S}{\partial z} = 0$

In industrial plants and particularly chemical reactors, the pressure drop is a serious problem. The radial flow spherical and tubular packed bed reactors possess lower pressure drops compared with the conventional axial flow reactors. Lower required material thickness is another major advantage of the spherical reactor compared with those of the tubular axial flow reactors. Hartig *et al.* studied methanol production in a spherical packed bed reactor [21]. They concluded that, this type of reactors were economically more desirable compared to tubular ones. Guillermo *et al.* presented a spherical reverse flow reactor for catalytic combustion of propane [22]. They determined the influence of the main operational and design parameters and the potential applications for this reactor. Rahimpour and co-workers optimized the methanol production in the multi-stage spherical reactors [23]. Their simulation results showed that, the case of two-stage configuration had the better performance compared to other alternatives such as single-stage, three-stage spherical and conventional tubular configurations. The modeling and simulation of the DME synthesis through methanol dehydration in the radial flow spherical reactor configurations based upon the mass and energy governing equations were performed by Farsi *et al.* [24]. Commercially, the tubular reactors are used in DME plants, while these reactors might be substituted by multi-stage spherical configuration to enhance the DME production and decreasing fixed operational costs. They concluded that, the conventional reactor might have been substituted by one, two or three spherical reactors. Then, the performance of multi-stage configurations compared with the conventional reactor under similar specifications. In this venue, lower pressure drops resulted in the higher DME production extents as well as lower manufacturing costs. All these suggested the optimized spherical bed reactors to be utilized instead of the conventional reactors to produce DME [24]. Rather than other

methods, syngas to DME conversion is easier and more efficient to perform in a simple slurry reactor. This enables; i) maintaining of a uniform temperature throughout the reactor, which is important for highly exothermic reactions; ii) easy handling that is important for addition and removal of catalyst to the reaction medium and iii) good temperature control, which prevents catalyst sintering [25]. Although a 5 and 100 tons/day slurry pilot plant was built in Japan, no commercial-scale syngas to DME conversion has been reported to date [26] and literature information on the simulation and design of industrial DME synthesis reactors is very scarce.

Therefore, in the current study, a mathematical model incorporating homogeneous and heterogeneous hydrodynamic models was developed and compared with a pilot plant experimental data available in the literature. Then, the effects of temperature and pressure on the CO conversion as well as DME production, and optimum values of the feed gas composition and reactor dimensions were investigated. In this model the energy balance was ignored due to the fact that, the temperature of the slurry reactor utilizing cooling water tubes remained constant throughout the process.

2. Mathematical modelling

The mathematical model for description of the homogeneous as well as heterogeneous gas flow based upon dispersion model for three-phase (*i.e.*; small bubbles, large bubbles and slurry phase) and catalyst particle sedimentation are presented in Table 1.

The empirical correlations for the gas hold up, volumetric mass transfer coefficient, superficial gas velocity of small bubbles, hindered sedimentation velocity of particles, dispersion coefficient of small and large bubbles, liquid and slurry velocity, gas solubility in paraffin liquid for prediction of the DME production and CO conversion in a large-scale slurry bubble column reactor

were obtained from references available in the open literature [27-36].

In the present study, kinetics of the methanol synthesis, Carbon dioxide hydrogenation and DME synthesis as independent reactions were taken from the work of Liu et al. [26] and provided as follows:

$$r_{CO} = A_1 \exp\left(-\frac{A_2}{RT}\right) f_{CO}^{A_3} f_{H_2}^{A_4} \left(1 - \frac{f_M}{K_{f_1} f_{CO} f_{H_2}^2}\right) \quad (5)$$

$$r_{CO_2} = A_5 \exp\left(-\frac{A_6}{RT}\right) f_{CO}^{A_7} f_{H_2}^{A_8} \left(1 - \frac{f_M f_w}{K_{f_2} f_{CO_2} f_{H_2}^3}\right) \quad (6)$$

$$r_D = A_9 \exp\left(-\frac{A_{10}}{RT}\right) f_M^{A_{11}} \left(1 - \frac{f_w f_D}{K_{f_3} f_M^2}\right) \quad (7)$$

3. Results and Discussion

The reactor operating conditions were listed in Table 2. The mathematical model was solved by the MATLAB software 2010a.

Figure 1 indicated the parity of CO conversion and DME production or STY (*i.e.*; the DME production rate per catalyst weight) for comparing the two hydrodynamic models (*i.e.*; homogeneous vs. heterogeneous) with experimental pilot plant data [37]. It might be seen from this figure that the prediction of the plant data for heterogeneous gas flow model was more accurate than that of the homogeneous one and the average relative deviations (ARD) of the former was lower than the latter one. The heterogeneous model predicted the CO conversion and DME production with ARD of 6.35% and 4.65%, respectively. Hence, in this paper for investigation of the effects of operating parameters the heterogeneous gas flow model was undertaken.

Figure 2 illustrated the effect of temperature on CO conversion and DME production in a large-scale bubble column slurry reactor. It is seen that, increasing the temperature led to the enhancement of the CO conversion and DME productivity due to the fact that increasing temperature accelerated methanol synthesis, CO

hydrogenation and methanol dehydration reactions. In addition, at higher temperatures the mass transfer coefficient and the solubility of the syngas in the slurry phase increased which meant that, the mass transfer resistance was lowered. However, it is reminded that the temperature may reach to limited heights due to the fact that all reactions in the direct DME synthesis were exothermic. Furthermore, at higher temperatures sintering phenomenon might have occurred which in turn could have resulted in reduced catalytic activity. Considering all these together, it is clear from this figure that the optimum value for the operating temperature was chosen to be 265°C.

Previous results of these authors' studies indicated [38,39] that, the axial temperature profiles from bottom to top of the slurry reactor changed very little related to that of a high heat capacity of the paraffin liquid as well as desirable heat carrying characteristics. Therefore, the direct DME synthesis via the syngas and carbon dioxide in a slurry reactor might be considered as an isothermal process. Also, it might be concluded from this figure that; the hot region for this system situated at top heights and above bottom of the slurry part of the reactor due to the catalyst grain sedimentation and high syngas partial pressure. This led to an increased methanol synthesis and dehydrogenation rates in turn causing more heat generation. Furthermore, results demonstrated that, the variation of temperature along the reactor length at higher operating temperatures was smaller than that of lower temperature values. In the other words, it might be a foregone conclusion that, at fixed cooling water and high slurry temperatures the driving force for the heat removal was higher than that of the state at which the reactor operated at lower temperatures. Therefore, the heat loss was high hence, the slurry temperature became uniform. This discussion led these authors towards the point that, no notable difference between the isothermal and non-isothermal reactors might be expected. In

the other words, the report of the temperature of 265°C as the isothermal and optimum condition value along the reactor

height seemed reasonable with a high degree of confidence.

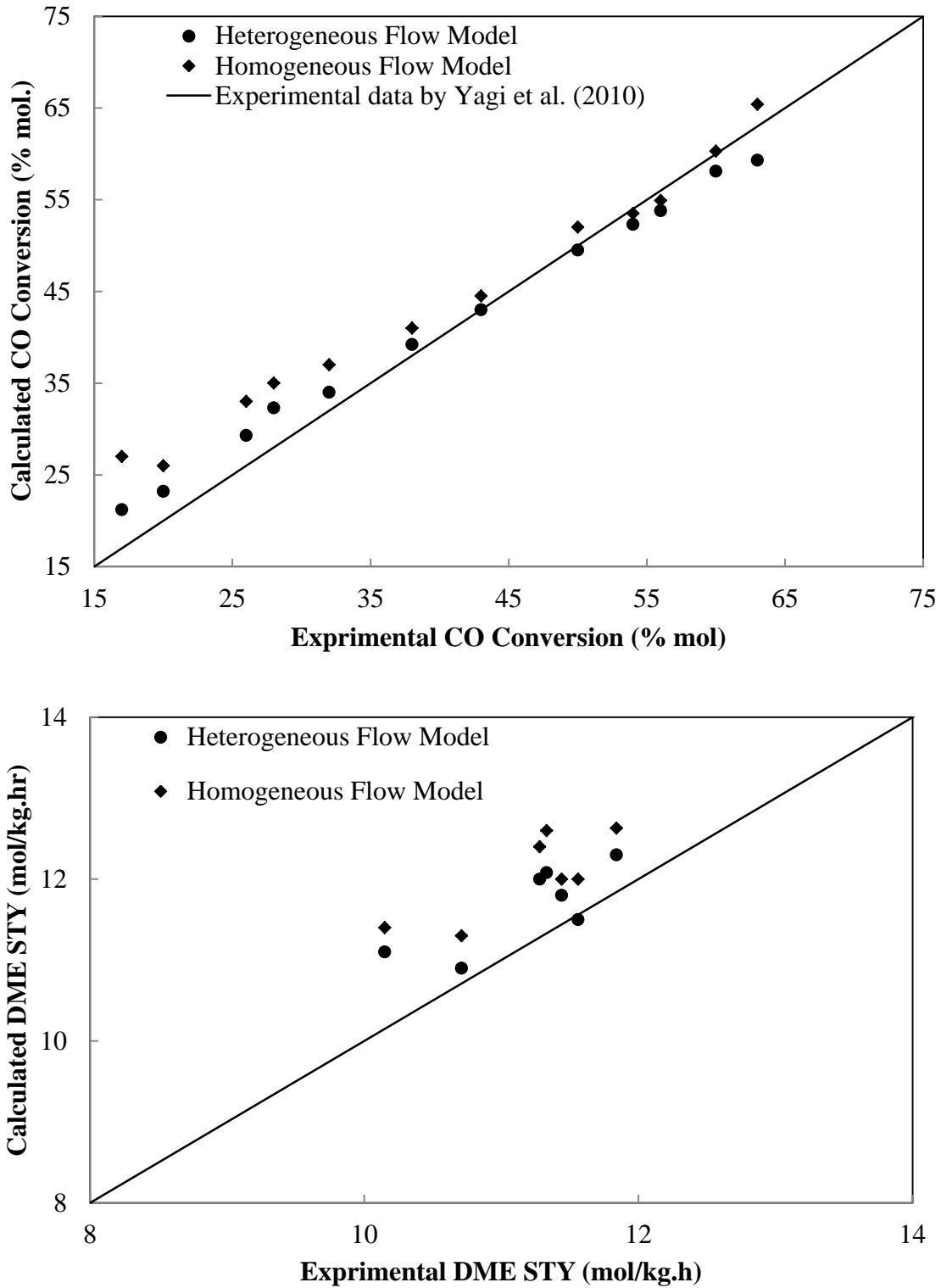


Figure 1: A comparison between the homogeneous and heterogeneous dispersion model with experimental pilot plant data

Table 2: Operating condition of bubble column slurry reactor

Volume of reactor	Temperature range	Pressure range	Superficial gas velocity	Mass of catalyst	Mass of paraffin	Feed gas composition $\frac{H_2 - CO_2}{CO + CO_2}$	Number of cooling pipes (size)
160 m ³	240-265°C	4-6 MPa	0.22 $\frac{m}{s}$	34.46 ton	68 ton	1-2	400 (38 mm)

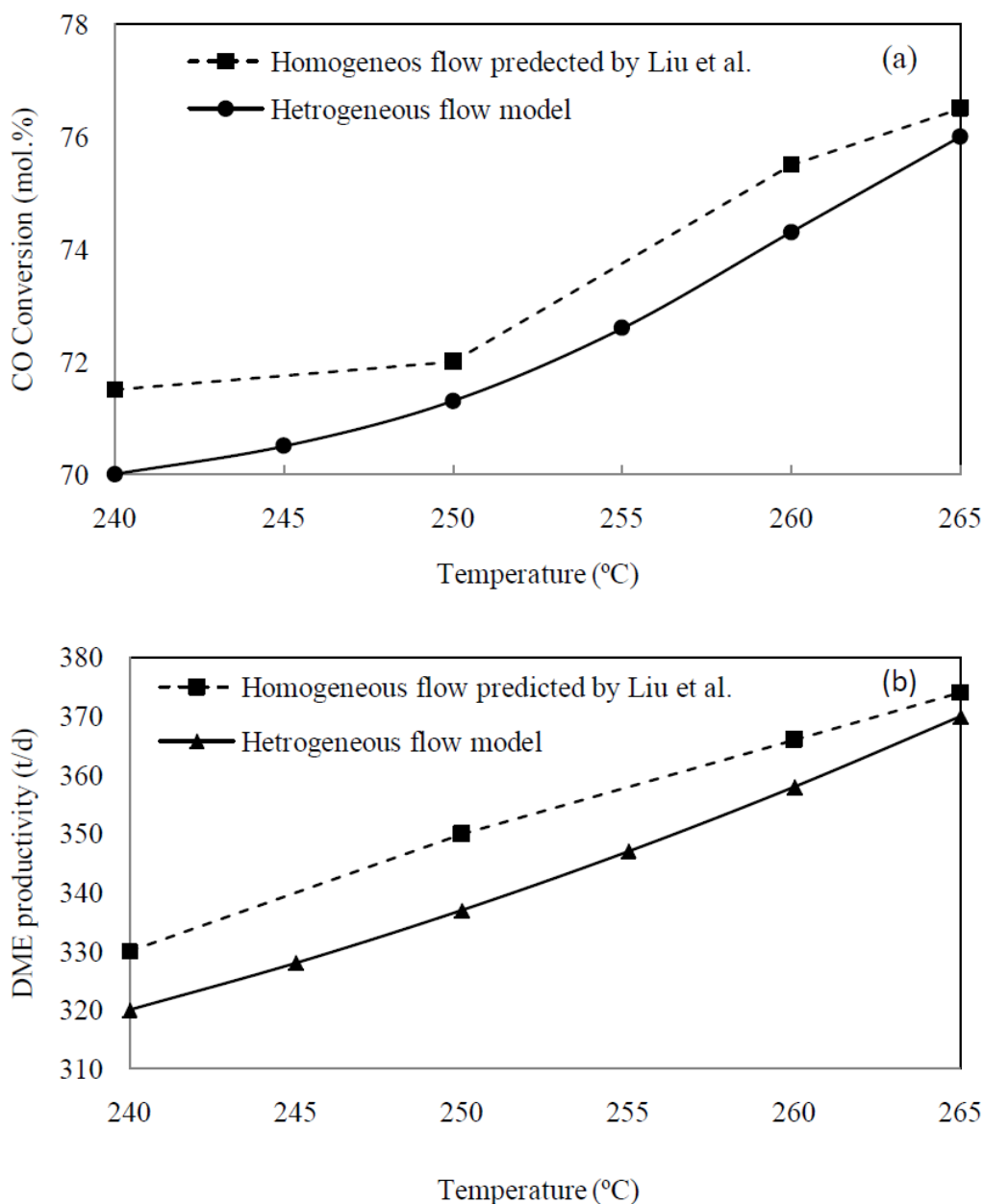


Figure 2: CO conversion and DME productivity vs. temperature: P = 6MPa, W/F = 11 (g-cat. h/mol), $\epsilon_s = 0.33$ wt. %, $U_G = 0.22$ m/s

Figure 3 showed the effect of pressure on the CO conversion. The results indicate that the increasing the operating pressure

redounds in improvement of CO conversion. The enhanced performance of the reactor might interpret in terms of the

carbon dioxide and methanol synthesis being mole-reducing reactions. Besides, the water gas shift and DME synthesis reactions had similar number of moles on both sides of reactions. Therefore, the increased operating pressure had positive effect on the CO conversion and DME production. Furthermore, the increased operating pressure led to enhancement of the mass transfer area which followed by increased volumetric mass transfer coefficient. Although increased pressure corresponded to the improved reactor performance, running reactions at high pressures was also limited by high operating costs. Therefore, a pressure of 50bar was selected as the optimum operating pressure for the direct DME synthesis. Moreover, higher syngas partial pressure at the inlet of the slurry reactor resulted in higher methanol synthesis rate in turn led to an enhancement of the methanol dehydration rate. Also, as mentioned earlier, the slurry temperature in this reactor hit a maximum value attributed to the high methanol synthesis and dehydrogenation rates.

Based upon these researchers previous studies [38,39], the enhancement of the superficial gas velocity led to lowering of the slope of the catalyst concentration versus the reactor height. This issue was attributed to the increasing of the slurry recirculation. In the other words, through rising of the recirculation of the slurry phase, the behavior understudied tended towards a perfectly mixed model. In addition, those previous results revealed that, the increased reactor diameter or decreased reactor height caused in more slurry recirculation hence, less sedimentation of catalyst. So, the slurry phase in the bubble column might have been considered as a perfectly mix reactor. Ultimately, results of homogeneous versus heterogeneous phase for prediction of the optimum values of reactor dimensions and feed gas composition were similar. Optimum value of the reactor diameter and height were thus, determined to be 3.2 and

20 meters, respectively and the best feed gas composition $\left(\frac{H_2-CO_2}{CO+CO_2}\right)$ for maximum conversion obtained to be 2.

4. Conclusions

In the present study, homogeneous and heterogeneous gas flow models developed and compared to an actual experimental pilot plant data. It was concluded that the heterogeneous model was more accurate for prediction of such plant information. Then effects of pressure and temperature on the CO conversion and DME productivity in a large-scale bubble column slurry reactor were investigated, also the optimum values for these operating conditions determined. Moreover, the results demonstrated a very insignificant difference between the homogeneous and heterogeneous approaches for prediction of optimum values of the feed gas composition and reactor dimensions. The investigation of temperature variation profiles and a comparison between the isothermal and non-isothermal reactor behaviors revealed that, the slurry bubble column reactor might be considered isothermal with rather small error incorporated into the simulation. In addition, the results of dispersion model indicated that, with the lowering of the reactor aspect ratio from the temperature and pressure point of view, the slurry phase might to be considered as a well mixed reactor. The CO conversion and DME production were demonstrated to rise with enhanced temperatures up to 265°C. Beyond this value, due to highly exothermic nature of reactions involved, the values of these chemical kinetics' parameters lowered. On the other hand, the rising pressure values enhanced the reactor performance. Ultimately, it is reminded that the developed model in this research might very well be applicable for designing of other large-scale slurry bubble column reactors so far as the chemical kinetics undertaken is known.

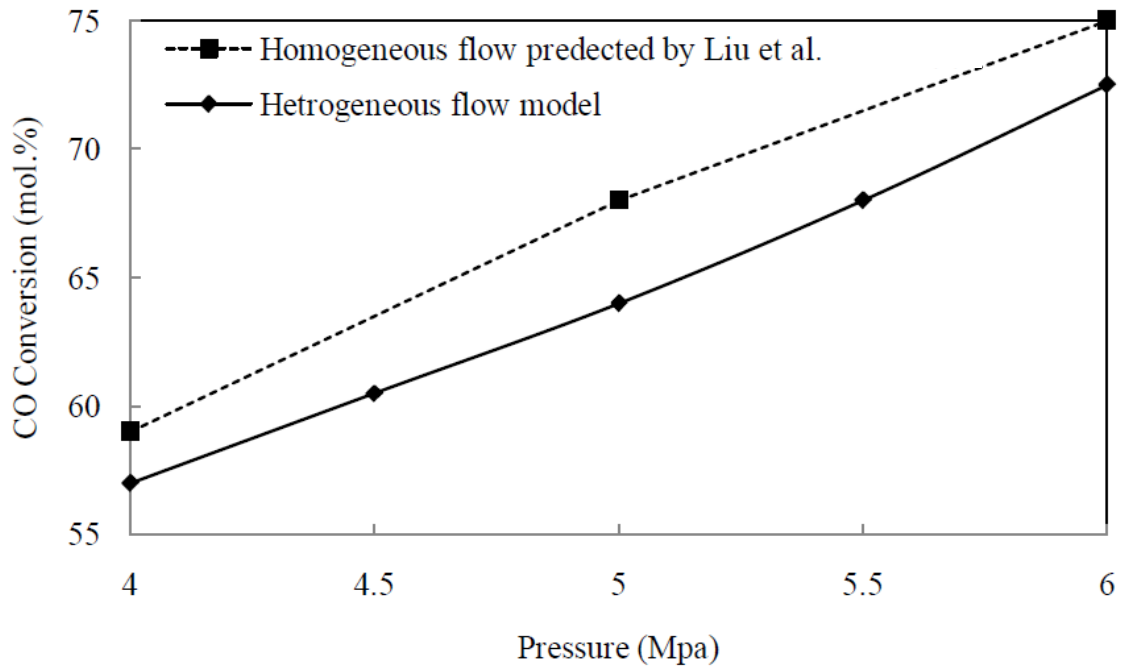


Figure 3: CO conversion along with the pressure: $T=260^{\circ}\text{C}$, $W/F = 11$ (g-cat. h/mol), $\varepsilon_s = 0.33$ wt. %, $U_G = 0.22$ m/s

Nomenclature

r_{CO}, r_{CO_2}, r_D	Intrinsic kinetics rate of carbon monoxide, carbon dioxide and dimethyl ether, (mol./hr.g-cat))
L	Reactor height, (m)
D_R	Reactor diameter, (m)
P	Operating pressure, (MPa)
T	Reaction temperature, (K)
R	Gas constant, ($\frac{J}{mol.K}$)
$C_{j,LB}$	Molar concentration of j component in large bubble phase, (mol/m ³)
$C_{j,SB}$	Molar concentration of j component in small bubble phase, (mol/m ³)
$C_{j,SL}$	Molar concentration of j component in slurry phase, (mol/m ³)
C_s	Catalyst concentration, (kg/m ³)
C_j^*	Equilibrium molar concentration in liquid, (mol/m ³)
$(k_1\alpha)_{LB}$	Volumetric mass transfer coefficient for large bubbles, (1/s)
$(k_1\alpha)_{SB}$	Volumetric mass transfer coefficient for small bubbles, (1/s)
k_{f1}	Rate constant of methanol synthesis
k_{f2}	Rate constant of carbon dioxide hydrogenation
k_{f3}	Rate constant of methanol dehydration
P_{CO}	Partial pressure of CO, MPa
P_{H_2}	Partial pressure of H ₂ , MPa
P_{CO_2}	Partial pressure of CO ₂ , MPa
P_M	Partial pressure of methanol, MPa
P_w	Partial pressure of water, MPa
M_{cat}	Mass of catalyst, (kg)
U_{LB}	Superficial velocity of large bubbles, (m/s)
U_{SB}	Superficial velocity of small bubbles, (m/s)
U_{SL}	Superficial velocity of slurry phase, (m/s)
U_{SL}	Inlet superficial velocity of slurry phase, (m/s)
U_G	Superficial gas velocity, (m/s)
U_{CO}	Inlet superficial gas velocity, (m/s)

U_p	Hindered sedimentation velocity, (m/s)
D_j	Diffusion coefficient, (m ² /s)
E_{LB}	Large bubble dispersion coefficient, (m ² /s)
E_{SB}	Small bubble dispersion coefficient, (m ² /s)
E_{SL}	Slurry phase dispersion coefficient, (m ² /s)
Greek symbols	
ε_{SB}	Small bubbles gas holdup
ε_G	Total gas holdup
ε_{LB}	Large bubbles gas holdup
ε_S	Solid concentration
v_{ij}	Reaction coefficient

References:

- 1- Semelsberger, T.A., Borup, R.L., Greene, H.L. (2005). "Dimethyl ether (DME) as an alternative fuel." *J. Power Sources*, No. 156, pp. 497-511.
- 2- Ng, K.L., Chadwick, D. and Toseland, B.A. (1999). "Kinetics and modelling of dimethyl ether synthesis from synthesis gas." *Chem Eng Sci*, No. 54, pp. 3587-3592.
- 3- Sosna, M.Kh., Sokollinskii, Yu.A., Shovkoplyas, N.Yu. and Korolev, E.V. (2007). "Application of the thermodynamic method to developing the process of producing methanol and dimethyl ether from synthesis gas." *Theor Found Chem Eng*, No. 41, pp. 809-815.
- 4- Wang, W., Wang, S., Ma, X. and Gong, J. (2011). "Recent advances in catalytic hydrogenation of carbon dioxide." *Chem Soc Rev*, No. 40, pp. 3703-3727.
- 5- An, X., Zuo, Y.-Z., Zhang, Q., Wang, D.-z. and Wang, J.-F. (2008). "Dimethyl ether synthesis from CO₂ hydrogenation on a CuO-ZnO-Al₂O₃-ZrO₂/HZSM-5 bifunctional catalyst." *Ind Eng Chem Res*, No. 47, pp. 6547-6554.
- 6- Bulushev, D.A., Ross, J.R.H., (2011), "Catalysis for conversion of biomass to fuels via pyrolysis and gasification." *Rev Cataly Today*, No. 171, pp. 1-13.
- 7- Ereña, J., Garoña, R., Arandes, J., Aguayo, M. A.T. and Bilbao, J. (2005). "Direct synthesis of dimethyl ether from (H₂+CO) and (H₂+CO₂) feeds. Effect of feed composition." *Int J Chem React Eng*, No. 3(1), p. A44.
- 8- Ereña, J., Garoña, R., Arandes, J.M., Aguayo, A.T. and Bilbao, J. (2005). "Effect of operating conditions on the synthesis of dimethyl ether over a CuO-ZnO-Al₂O₃/NaHZSM-5 bifunctional catalyst." *Catal Today*, No. 107-108, pp. 467-473.
- 9- Flores, J.H., Peixoto, D.P.B., Appel, L.G., de Avillez, R.R. and Pais da Silva, M.I. (2011). "The influence of different methanol synthesis catalysts on direct synthesis of DME from syngas." *Catal Today*, Vol. 172, pp. 218-225.
- 10- Stiefel, M., Ahmad, R., Arnold, U. and Döring, M. (2011). "Direct synthesis of dimethyl ether from carbon-monoxide-rich synthesis gas: Influence of dehydration catalysts and operating conditions." *Fuel Process Technol*, No. 92, pp. 1466-1474.
- 11- Ereña, J., Sierra, I., Olazar, M., Gayubo, A.G. and Aguayo, A.T. (2008). "Deactivation of a CuO-ZnO-Al₂O₃/γ-Al₂O₃ catalyst in the synthesis of dimethyl ether." *Ind Eng Chem Res*, No. 47, pp. 2238-2247.

- 12- Sierra, I., Ereña, J., Aguayo, A.T., Olazar, M. and Bilbao, J. (2010). "Deactivation kinetics for direct dimethyl ether synthesis on a CuO-ZnO-Al₂O₃/γ-Al₂O₃ catalyst." *Ind Eng Chem Res*, No. 49, pp. 481-489.
 - 13- Sierra, I., Ereña, J., Aguayo, A.T., Arandes, J.M. and Bilbao, J. (2010). "Regeneration of CuO-ZnO-Al₂O₃/γ-Al₂O₃ catalyst in the direct synthesis of dimethyl ether." *Appl Catal B: Environ*, No. 94, pp. 108-116.
 - 14- Fazlollahnejad, M., Taghizadeh, M., Eliassi, A., Bakeri, G. (2009). "Experimental study and modeling of an adiabatic fixed-bed reactor for methanol dehydration to dimethyl ether." *Chin J Chem Eng*, No. 17, pp. 630-634.
 - 15- Farsi, M., Eslamlueyan, R., Jahanmiri, A. (2011). "Modeling, simulation and control of dimethyl ether synthesis in an industrial fixed-bed reactor." *Chem Eng Process: Process Intens*, No. 50, pp. 85-94.
 - 16- Farsi, M., Mazinani, S., Jahanmiri, A. (2011). "Steady state operability characteristics of an adiabatic fixed-bed reactor for methanol dehydration." *Iran J Chem Chem Eng*, No. 30, pp. 45-50.
 - 17- Farsi, M., Jahanmiri, A. (2011). "Enhancement of DME production in an optimized membrane isothermal fixed-bed reactor." *Int J Chem React Eng*, No. 9, p. A74.
 - 18- Farsi, M., Jahanmiri, A., Eslamloueyan, R. (2010). "Modeling and optimization of MeOH to DME in isothermal fixed-bed reactor." *Int J Chem React Eng*, No. 8, p. A79.
 - 19- Omata, K., Ozaki, T., Umegaki, T., Watanabe, Y., Nukui, N., Yamada, M. (2003). "Optimization of the temperature profile of a temperature gradient reactor for DME synthesis using simple genetic algorithm assisted by a neural network, high-quality transportation fuels." *Energ Fuel*, No. 17, pp. 836-841.
 - 20- Kordabadi, H., Jahanmiri, A. (2005). "Optimization of methanol synthesis reactor using genetic algorithms." *Chem Eng J*, No. 108, pp. 249-255.
 - 21- Hartig, F., Keil, F.J. (1993). "Large-scale spherical fixed bed reactors." *Ind Eng Chem Res*, No. 32, pp. 424-437.
 - 22- Viecco, G.A., Caram, H.S. (2002). "The spherical reverse flow reactor." *Chem Eng Sci*, No. 57, pp. 4005-4025.
 - 23- Rahimpour, M.R., Abbasloo, A., Sayyad Amin, J. (2008). "A novel radial-flow, spherical-bed reactor concept for methanol synthesis in the presence of catalyst deactivation." *Chem Eng Technol*, No. 31, pp.1615-1629.
 - 24- Farsi, M., Asemani, M., Rahimpour, M.R. (2014). "Mathematical modeling and optimization of multi-stage spherical reactor configurations for large scale dimethyl ether production." *Fuel Process Technol*, No. 126, pp. 207-214.
 - 25- Chen, Z., Zhang, H., Ying, W., Fang, D. (2010). "Study on direct alcohol/ether fuel synthesis process in bubble column slurry reactor." *Front Chem Eng*, No. 4, pp. 461-471.
 - 26- Liu, D., Hua, X., Fang, D. (2007). "Mathematical simulation and design of three-phase bubble column reactor for direct synthesis of dimethyl ether from syngas." *J Nat Gas Chem*, No. 16, pp.193-199.
 - 27- Maretto, C., Krishna, R. (1999). "Modelling of a bubble column slurry reactor for Fischer-Tropsch synthesis." *Catal Today*, No. 52, pp. 279-289.
 - 28- Maretto, C., and Krishna, R. (2001). "Design and optimisation of a multi-stage bubble column slurry reactor for Fischer-Tropsch synthesis." *Catal Today*, No. 66, pp. 241-248.
-

- 29- Reilly, I.G., Scott, D.S., W Debruijn, T.J., Macintyre, D. (1994). "The role of gas phase momentum in determining gas holdup and hydrodynamic flow regimes in bubble column operations." *Can J Chem Eng*, No. 72, pp. 3-12.
 - 30- Krishna, R., De Swart, J.W.A., Ellenberger, J., Martina, G.B., Maretto, C. (1997). "Gas holdup in slurry bubble columns: Effect of column diameter and slurry concentrations." *AIChE J*, No. 43, pp. 311-316.
 - 31- Vermeer, D.J., Krishna, R., (1981). "Hydrodynamics and mass transfer in bubble columns operating in the churn-turbulent regime." *Ind Eng Chem Des Deve*, No. 20, pp. 475-482.
 - 32- Smith, D.N., Ruether, J.A. (1985). "Dispersed solid dynamics in a slurry bubble column." *Chem Eng Sci*, No.40, pp.741-753.
 - 33- De Swart, J.W.A., van Vliet, R.E., Krishna, R. (1996). "Size, structure and dynamics of "large" bubbles in a two-dimensional slurry bubble column." *Chem Eng Sci*, No. 51, pp.4619-4629.
 - 34- Field, R.W., Davidson, J.F. (1980) "Axial dispersion in bubble columns." *T I Chem Eng*, No. 58, pp. 228-235.
 - 35- Deckwer, W.-D., Schumpe, A. (1993). "Improved tools for bubble column reactor design and scale-up." *Chem Eng Sci*, No. 48, pp. 889-911.
 - 36- Wang, T., Wang, J. "Numerical simulations of gas-liquid mass transfer in bubble columns with a CFD-PBM coupled model." *Chem Eng Sci*, No. 62, pp. 7107-7118.
 - 37- Yagi, H., Ohno, Y., Inoue, N., Okuyama, K., Aoki, S. (2010). "Slurry phase reactor technology for DME direct synthesis." *Int J Chem React Eng*, No. 8, p. A109.
 - 38- Papari, S., Kazemeini, M., Fattahi, M. (2012). "Mathematical modeling of a slurry reactor for DME direct synthesis from syngas." *J Nat Gas Chem*, No. 21, pp. 148-157.
 - 39- Papari, S., Kazemeini, M., Fattahi, M. (2013). "Modelling-based optimisation of the direct synthesis of dimethyl ether from syngas in a commercial slurry reactor." *Chinese J Chem Eng*, No. 21, pp. 611-621.
-